

Ordering of Time-Difference Data From Multispectral Imagery

PAUL SWITZER

Department of Statistics, Stanford University, California 94305

S. E. INGBRITSEN*

Department of Applied Earth Sciences, Stanford University, California 94305

Our goal is to exhibit multispectral time-difference data in factored form so as to emphasize signal differences, assumed to be spatially structured, and isolate noise, which is assumed to be spatially unstructured. The method we use is a variant of the MAF procedure (Min/Max Autocorrelation Factors), a general purpose technique which extracts p orthogonal linear combinations or factors of the p -variate data which have maximal to minimal spatial autocorrelation. We discuss the application of MAF to time-difference imagery, and present three examples. The first two examples were generated from Landsat MSS image pairs and the third from Daedalus airborne scanner imagery.

Introduction

A number of authors (Lodwick, 1979; 1981; Byrne et al., 1980; Richards, 1984; Ingebritsen and Lyon, 1985) have applied standard principal components analysis (PCA) to the problem of detecting and classifying temporal change in remotely sensed imagery. Each of these studies involved geographically registered Landsat multispectral scanner (MSS) imagery. Lodwick (1979) looked at seasonal changes using the first two principal components (PCs), by differencing the PC scores between images or by using linear regression across a number of images. Byrne et al. (1980) treated two Landsat MSS images of the same area as a single eight-channel data set, and noted that PCA of the augmented data set generated higher order PCs that contained information about temporal change.

Richards (1984) used the same method and reported similar results.

Ingebritsen and Lyon (1985) showed that the method of Byrne et al. often leads to specific types of change-related PCs, which they referred to as " Δ brightness" and " Δ greenness" in analogy to Kauth and Thomas' (1976) "brightness" and "greenness." They noted, however, that the apparent success of this method in distinguishing separate "stable" and "change" components is largely a function of the restricted dimensionality of Landsat MSS data, rather than the method itself. The method is not expected to be generally effective, and fails to take advantage of the data-compression and ordering properties of PCA because it does not operate directly on the time-change data.

We suggest applying PCA and the Min/Max Autocorrelation Factors (MAF) process (Switzer and Green, 1984) directly to time-difference imagery. Either standard PCA or the MAF process can be

*Now at U.S. Geological Survey, Menlo Park, CA 94025.

used to order and reduce multispectral time-change information. Standard PCA produces decorrelated variables that are ordered based on a simple variance criterion, while the MAF process produces decorrelated variables that are ordered according to the degree of spatial autocorrelation. Since noise is commonly associated with low spatial autocorrelation, MAF provides a method for noise separation which is more rational than the variance criterion associated with standard PCA. A brief description of MAF is given in the next section.

MAF reduces to standard PCA when the multiband noise vector is proportional to the identity matrix; that is, when there is constant noise variance in all channels of the time-difference image and uncorrelated noise between channels. Typically it is difficult to know when this property obtains because the noise components of the data are not separately observable. However, for multispectral systems in which all frequency bands have the same noise variance (e.g., Landsat MSS) the PCA and MAF solutions generally are similar.

Since the MAF procedure is a generally effective method of isolating noise, and for the sake of brevity, we emphasize the MAF analysis in this paper. PC score images are produced in the course of the MAF algorithm, so it is straightforward to refer to both the PC and MAF images during interpretive processing.

Methodology

Let $\mathbf{Z}_1(x)$ denote the p -vector of energy measurements (gray levels) in P selected wavelength bands for a pixel at location x measured at time 1. Similarly let $\mathbf{Z}_2(x)$ denote the vector of energy

measurements at x measured at time 2. It will be immaterial whether or not these energy measurements have been previously rescaled (linearly) to give constant variance for each channel across the spatial domain D of interest, provided that the same rescaling has been applied at both times. Indeed, any fixed nonsingular matrix transformation of the p -variate field, e.g., to raw or rescaled factor scores, will not affect the final MAF results, *provided that the same transform has been applied to the images at both time points*. This property is obtained because we are dealing with a correlation rather than a variance criterion. Let

$$\mathbf{Z}_D(x) = \mathbf{Z}_2(x) - \mathbf{Z}_1(x),$$

where $\mathbf{Z}_D(x)$ is the p -variate time-difference field on the domain D . The goal is to exhibit this difference field in such a way as to emphasize the spatially structured signal differences and isolate the spatially unstructured noise. The method we use is a variant of the MAF procedure described in Switzer and Green (1984). The MAF procedure is a general purpose technique which extracts p orthogonal linear combinations or factors of the p -variate data which have maximal to minimal spatial autocorrelation.

The significant properties of the factors derived from MAF are as follows:

- i. The ordering of MAF factors is according to degree of spatial autocorrelation with the first factor having the maximum possible spatial autocorrelation and the last factor the minimum possible.
- ii. Unlike standard PCA, MAF factors are invariant to rescaling or other linear transformations of the data. In the case of time-differenced

imagery neither MAF nor the standard PCA is invariant when different rescalings are applied to the separate images at the two time points.

- iii. MAF reduces to the ordinary PCA only when the covariance matrix of the multichannel noise vector is proportional to the identity matrix.

The rationale for the application of MAF to time-difference spatial imagery is as follows: Those linear combinations of the p channels which had no signal change across the image between time 1 and time 2 should exhibit pure noise. We suppose that noise characteristically shows little spatial coherence; therefore, the minimal autocorrelation factor is taken to be an optimal representation of a pure noise component. Conversely, the signal change which has the greatest degree of spatial coherence should emerge as the maximal autocorrelation factor. The MAF algorithm is thus designed to separate noise from time changes on multiple-pixel scales.

Application

A computationally straightforward way to generate the MAF solution is as follows. First, perform a PC transformation on the time-difference data to produce uncorrelated equal-variance variables; second, operating on the PC score image, generate spatial covariance matrices based on horizontal and vertical shifts within that image; third, create a pooled spatial covariance matrix by computing the root mean square of the covariance matrices of step 2; and, finally, obtain the PC solution for the pooled covariance matrix. This is the MAF solution for the time-difference field.

There are two kinds of change which the MAF procedure will not detect. First, if the time change is a constant increment or decrement in the signal across the whole image, then this situation is indistinguishable to MAF from a zero increment, i.e., no signal change at all. Other methods will easily distinguish this case (e.g., simple differencing), but in fact such changes are commonly attributable to instrumental or atmospheric factors that are not of interest to the interpreter. Second, if the time change is spatially very spotty, i.e., only affecting isolated pixels or very small groups of pixels, then MAF will also have difficulty distinguishing this situation from the no-change situation. The absolute size of a changed area that could be "overlooked" by MAF is governed by (1) pixel size and (2) the size of the vertical and horizontal shifts used in the MAF algorithm. We generally use unit (1 pixel) shifts. A possible example is the detection of very small cleared areas against a forested background. However, if the spectral changes in such small areas are similar to those in larger changed areas—as will often be the case—the small areas will be identified along with the larger ones. It should also be noted that the MAF algorithm will not necessarily detect changes that are expressed only as an increase or decrease in spatial variability.

The same properties of MAF that make it possible to overlook spotty time change may be desirable in another respect. Difference images are in general extremely sensitive to misregistration, even when good registration accuracy is achieved. MAF should tend to identify misregistration effects in the time-difference field as noise, as they will generally have little spatial coherence.

MAF, like other multivariate methods of analysis, operates on covariance matrices. These are calculated globally for any image. However, since the definition of an image is arbitrary, one might calculate separate covariance matrices for subimages and produce a separate more particular analysis for each subimage. We have not explored this possibility in this paper.

In the examples below, the difference images and PC score images produced in the course of the MAF algorithm are compared with the MAF images. For interpretive purposes, and to facilitate comparison with standard PCA, it is useful to rotate the MAF solution vectors back into the original data space. This is a simple linear transformation, and in the examples below the MAF vectors are described in terms of the original data space.

Examples

We present three examples of MAF processed time-difference imagery. In

each case preprocessing steps included geographic registration of a 256×512 pixel subscene, resampling (using bicubic interpolation), and generation of a difference image. The difference data were normalized to unit variance. For some applications transformation of the raw data from each image to percent reflectance might be a useful additional step, as the MAF algorithm is potentially sensitive to differences in solar flux.

The first two examples are generated from Landsat MSS image pairs. The first is from an area in the Okanogan Highlands province of Washington State; the second is from the western Carson Desert, NV. MAF weights for these examples are given in Table 1, along with the results of standard PCA for comparison. In general, the maximal and minimal PCs are similar to the corresponding MAF factors, as expected for systems in which all frequency bands have the same noise variance (Switzer and Green, 1984). The Okanogan Highlands imagery (Fig. 1) includes the area in and around Midnite

TABLE 1 MAF and PCA Weights For the Landsat MSS Examples

		BAND 4	BAND 5	BAND 6	BAND 7
<u>Okanogan Highland Example</u>					
MAF weights	1	1.56	3.59	0.59	0.92
	2	-0.62	-1.32	2.15	2.64
	3	-0.79	-1.45	4.75	3.54
	4	4.96	4.82	-0.10	0.02
PC weights	1	0.31	0.32	0.32	0.24
	2	-0.46	-0.43	0.32	0.74
	3	-0.68	-0.21	1.86	1.34
	4	-2.10	2.30	-0.37	0.18
<u>Carson Desert Example</u>					
MAF weights	1	-0.72	-1.48	0.71	2.20
	2	1.12	0.44	0.28	0.00
	3	0.14	-1.58	3.88	2.72
	4	-3.34	3.10	1.09	0.93
PC weights	1	0.27	0.28	0.28	0.26
	2	-0.73	-0.61	0.43	0.93
	3	-2.40	3.04	1.51	0.87
	4	-1.88	0.82	3.23	2.45

DIFFERENCE IMAGE

MAF PROCESSING OF DIFFERENCES

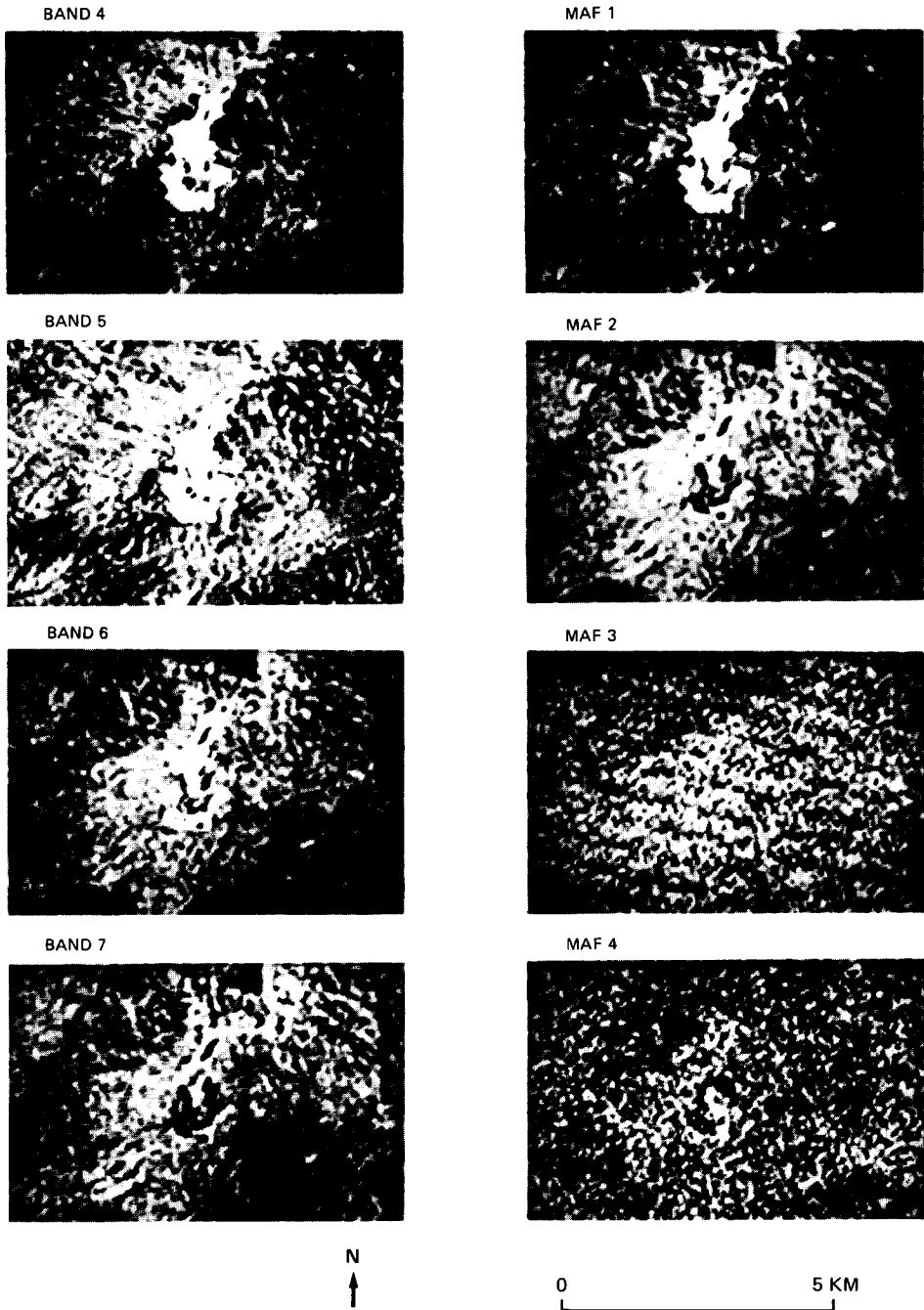


FIGURE 1. Landsat MSS example from the Okanogan Highlands, WA. Difference images are shown on the left, and MAF results on the right. The basic structure of the time change is clear in the unfactored difference images, and MAF simply reveals the true dimensionality.

Mine, a large open pit uranium mine. The images used in this example were acquired 8 August 1973 and 29 July 1980. Changes between the two dates are related primarily to expansion of the mine area, differences in the condition of the vegetation, and soil moisture differences.

MAF 1 shows the area of expansion as an anomalously bright area in the center of the image. The area that had been mined by 1973 is the roughly horseshoe-shaped area of moderate tone encircled by the area of expansion. Although MAF 1 and PC 1 are very similar, MAF 1 distinguishes the area of expansion more explicitly. The loading pattern for PC 1 is relatively uniform, while MAF 1, [1.56 3.59 0.55 - 0.92], is most heavily weighted on the bands in which the area of expansion is most distinct from its surroundings (see Fig. 2). Thus maxi-

mal autocorrelation is obtained by emphasizing the differences between the area of expansion and the remainder of the image, allowing the area to be mapped as two large, spectrally distinct, relatively homogeneous units. Because MAF 1 has the property of maximal autocorrelation, it will tend to divide the time-difference field into a few broadly contrasting areas.

MAF 2, [-0.62 -1.32 2.15 2.64], is less straightforward to interpret. It is somewhat similar to PC 2, which clearly responds to changes in green biomass. Outside the mine area, MAF 2 also responds to changes in green biomass, but its map shows quite a bit of spatial variability in the mine area itself. A pond near the north end of the mine, within the area of expansion, appears as a dark anomaly, as does the pre-1973 mine area, perhaps due to greater soil moisture at

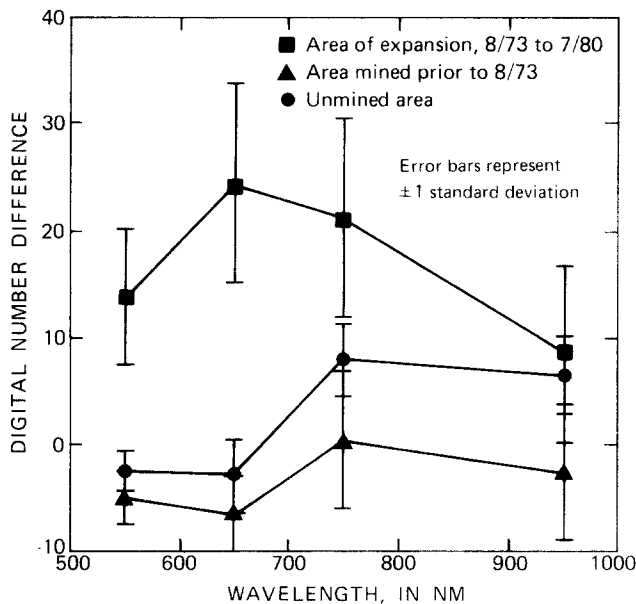


FIGURE 2. Selected spectra from the Okanogan Highlands difference image shown in Fig. 1: (■) area of expansion, 8/73-7/80; (▲) area mined prior to 8/73; (●) unmined area.

the time of the 1980 image. The area of expansion, aside from the pond, is moderate to bright in tone.

MAF 3 and MAF 4 contain little or no useful spatial information from an interpretive standpoint and represent the successfully isolated noise components. In this example the basic structure of the change is fairly evident from the unfactored difference imagery, and the MAFs simply reveal the true dimensionality. MAFs 3 and 4 are very similar to PCs 3 and 4; as anticipated, both methods apparently provide noise separation.

The Carson Desert imagery (Fig. 3) includes much of the wetland created by the terminal sink of the Carson River. The imagery used in the example was acquired 26 May 1973 and 6 August 1973. Change during this period was primarily related to a decline in water level, changes in green biomass, and the appearance and disappearance of salt efflorescence.

In this example, MAF 1 is very similar to PC 2 and MAF 2 is very similar to PC 1, i.e., the ordering with respect to the spatial criterion is different than the variance ordering.

MAF 1, $[-0.72 \quad -1.48 \quad 0.71 \quad 2.20]$, highlights areas that changed from shallow water to mudflats or moderately deep water to shallow water, and wetland areas where green biomass increased. The relatively few dark anomalies include some small ponds in which the amount of suspended sediment has decreased (near the Carson River distributary system, on the west side of the image), and areas outside the wetland where the amount of green biomass has decreased.

MAF 2, $[1.12 \quad 0.44 \quad 0.28 \quad 0.00]$, highlights areas that changed from mudflats or very shallow water to dry land, and areas where a salt crust developed. Areas

where salt efflorescence decreased or disappeared are shown as numerous and distinct dark anomalies.

As in the Okanogan Highlands examples, detector striping is enhanced by MAF 3 and MAF 4. In this case, however, MAF 3 also contains spatial information that is useful in interpretive processing, while MAF 4 generally isolates noise. MAFs 3 and 4 are only crudely similar to PCs 3 and 4.

The first two examples do not demonstrate the superiority of MAF with regard to isolating the noise component of the time-difference field, as they involve a system in which the frequency bands have equal noise variance, so that PCs and MAFs are roughly correlated. Generally, we would expect the degree of correlation between the two methods to decrease as the number of bands increases, as with more spectrally complicated data it becomes more likely that noise will have different statistical properties in different bands. Our final example allows the superior ordering and noise separation properties of the MAF method to be demonstrated.

This example was generated from a pair of Daedalus airborne scanner (AADS-1268) images of an area west of Palo Alto, California (Fig. 4). The band positions include the seven Thematic Mapper bands and four additional bands in the visible and near infrared. The imagery used in the example was acquired 23 April 1982 and 13 September 1983. Much of the area is within Stanford University's Jasper Ridge Biological Preserve, and changes visible in the imagery are largely related to natural seasonal changes in the vegetative cover.

In this example PCA of the time-difference data does not provide noise sep-

DIFFERENCE IMAGE

MAF PROCESSING OF DIFFERENCES

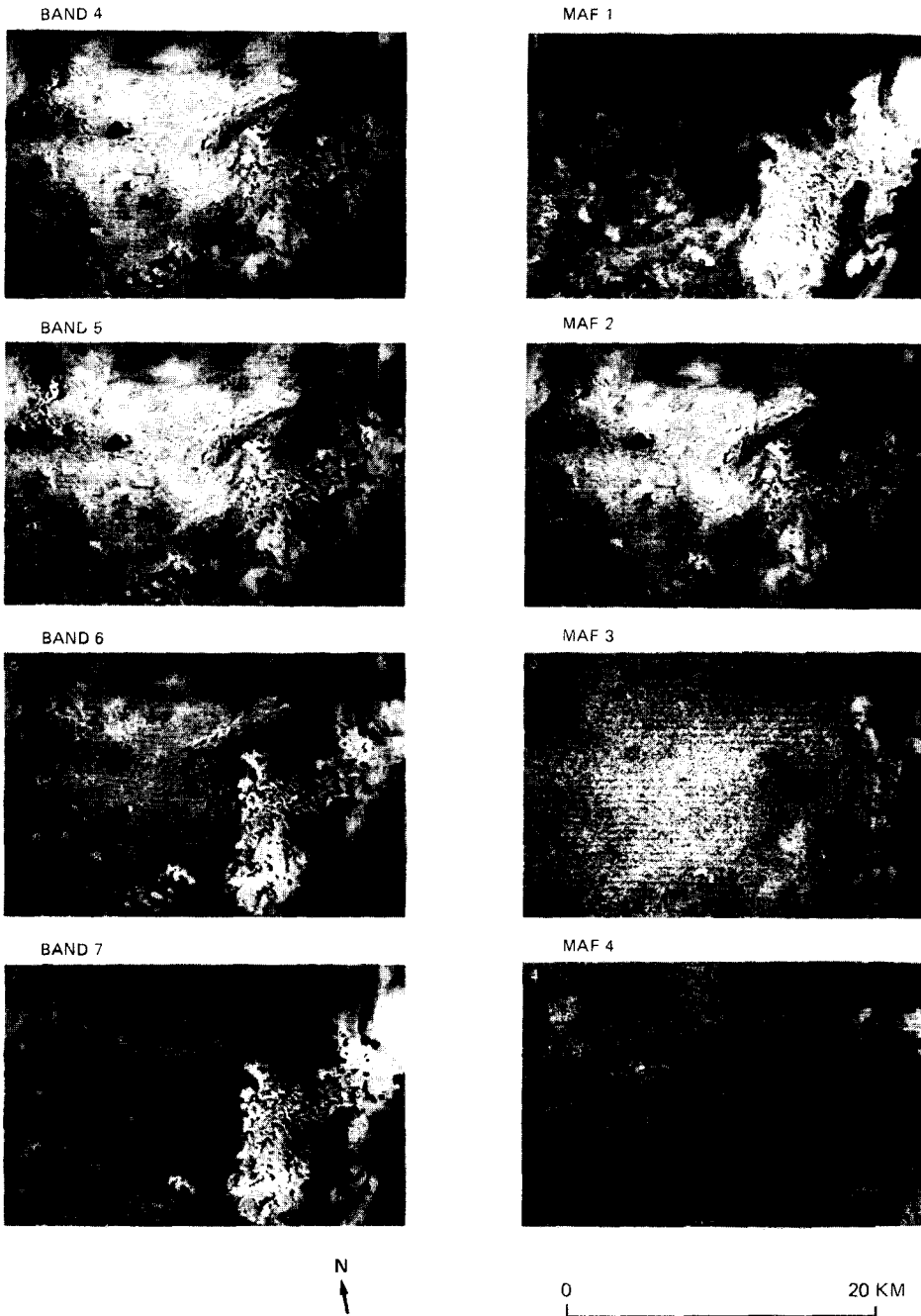


FIGURE 3. Landsat MSS example from the Carson Desert, NV. Difference images are shown on the left, and MAF results on the right.

PCA OF DIFFERENCES

MAF PROCESSING OF DIFFERENCES

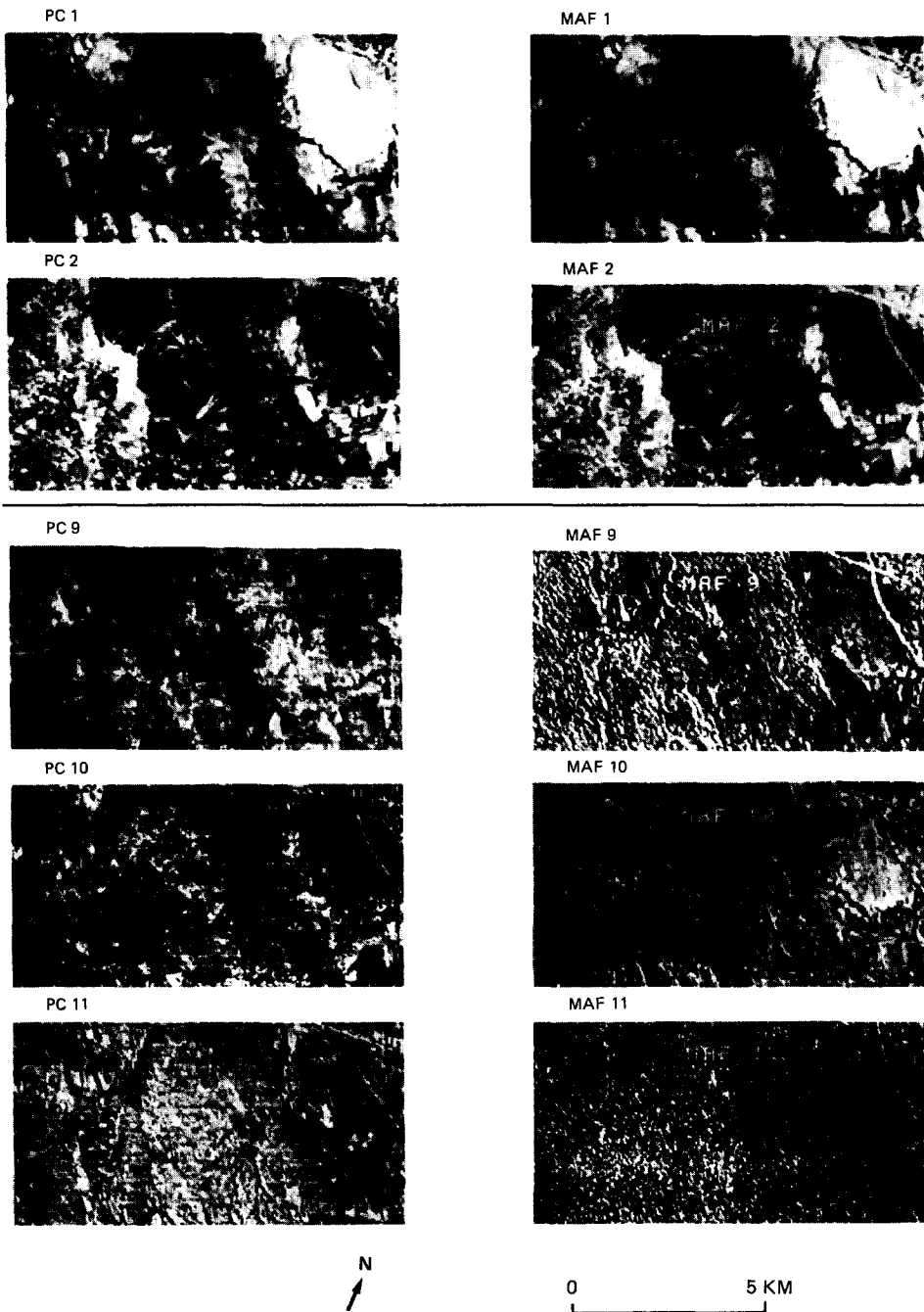


FIGURE 4. Example generated from Daedulus airborne scanner data acquired west of Palo Alto, CA. Results of PCA of the time-differenced field are shown on the left, MAF results on the right. Unlike PCA, MAF clearly isolates noise in the time-difference field.

aration. While there are several noisy PCs (e.g., PCs 9, 10, and 11—Fig. 4), there is no PC that clearly isolates noise. The MAF process, on the other hand, clearly isolates noise in the time–difference field (e.g., MAF 11—Fig. 4).

Summary

A number of authors have applied standard PCA to the change-detection problem. Byrne et al. (1980), Richards (1984), and Ingebritsen and Lyon (1985) all treated registered Landsat MSS image pairs as eight-band data sets, and performed PCA on the augmented data sets. This method is not expected to be generally effective, and fails to take advantage of the data-compression and ordering properties of PCA because it does not operate directly on the time–change data.

We suggest applying PCA and MAF process (Switzer and Green, 1984) directly to time–difference imagery, with the goal of separating the signal and noise components of the time–difference field. The MAF procedure is favored because (unlike standard PCA) it is a generally effective method of isolating noise.

Even in the case of low-dimensional data (e.g., Landsat MSS) the MAF algorithm described in this paper is useful in terms of clarifying the spatial structure of change and revealing the true dimensionality of time–change data. With more spectrally complex scanner imagery, the data compression properties of the method become more useful.

We would like to thank Professor R. J. P. Lyon for his encouragement of this study and for allowing us to use the image processing facilities of the Stanford Remote Sensing Laboratory. We would also like to thank three anonymous

referees for their helpful suggestions, and the staff at the NASA-Ames Research Center for providing the airborne scanner imagery. This work was prepared under the auspices of N. S. F. Grant MCS 81-09584. Rebecca Munn typed the manuscript.

References

- Byrne, G. F., Crapper, P. F., and Mayo, K. K. (1980), Monitoring land-cover change by principal components analysis of multitemporal Landsat data, *Remote Sens. Environ.* 10:175–184.
- Ingebritsen, S. E., and Lyon, R. J. P. (1985), Principal components analysis of multitemporal image pairs, *Int. J. Remote Sens.* 6:687–696.
- Kauth, R. J., and Thomas, G. S. (1976), The tasseled cap—a graphic description of the spectral-temporal development of agricultural crops as seen by Landsat, Proceedings of the Symposium on Machine Processing of Remotely Sensed Data, Purdue University, pp. 45–51.
- Lodwick, G. D. (1979), Measuring ecological changes in multitemporal Landsat data using principal components, Proceedings of the International Symposium on Remote Sensing of the Environment, Ann Arbor, MI, pp. 1131–1141.
- Lodwick, G. D. (1981), A computer system for monitoring environmental change in multitemporal Landsat data, *Can. J. Remote Sens.* 7:24–33.
- Richards, J. A. (1984), Thematic mapping from multitemporal image data using the principal components transformation, *Remote Sens. Environ.* 16:35–46.
- Switzer, Paul, and Green, A. A. (1984), Min/max autocorrelation factors for multivariate spatial imagery, Technical Report No. 6, Department of Statistics, Stanford University, 14 pp.

Received 25 November 1985; revised 31 March 1986.